MiR-16 Targets the Serotonin Transporter: A New Facet for Adaptive Responses to Antidepressants

Anne Baudry *et al.*

Science **329**, 1537 (2010);
DOI: 10.1126/science.1193692

early during translation, targeting actin for degradation in a proteasome-dependent or -independent way. However, replacement of Lys^{18} had only a partial effect in reducing the ubiquitination and stabilizing the arginylated γ-actin, suggesting that other Lys residues in the actin sequence or the molecular chaperones involved in cotranslational actin processing may also contribute to this process (*18*).

In addition to selective degradation, actin isoforms may also be selectively recognized by arginyltransferase, either via the specificity of the enzyme itself or by its spatial segregation toward one actin isoform. However, arginyltransferase has fairly poor substrate specificity (*7*), and it can efficiently arginylate both N-terminal Asp and Glu (*19*, *20*), found at the N terminus of β- and γ-actin, respectively (*5*). Spatial segregation toward one actin isoform is also unlikely, because arginyltransferase appears to have no relevant bias in its intracellular distribution (*19*, *20*). Actin's N-terminal acetylation (*5*, *21*, *22*) may also be isoform-biased and regulate its degradation state; however, to date all actin isoforms appear to be equally acetylated. Thus, selective degradation appears to be the most plausible explanation for why only one of the two predominant actin isoforms is arginylated in nonmuscle cells.

For some proteins, N-terminal arginylation targets them for degradation (*16*, *23*), whereas for others it does not (*7*, *8*). Perhaps arginylation may be a self-regulating modification that ensures selective accumulation of some arginylated proteins and removal of others. This mechanism may be used not only with actin isoforms but also with other closely homologous but selectively arginylated proteins.

References and Notes

1. C. A. Otey, M. H. Kalnoski, J. L. Lessard, J. C. Bulinski, *J. Cell Biol.* **102**, 1726 (1986).
2. C. A. Otey, M. H. Kalnoski, J. C. Bulinski, *J. Cell. Biochem.* **34**, 113 (1987).
3. D. Höfer, W. Ness, D. Drenckhahn, *J. Cell Sci.* **110**, 765 (1997).
4. J. Condeelis, R. H. Singer, *Biol. Cell* **97**, 97 (2005).
5. P. A. Rubenstein, D. J. Martin, *J. Biol. Chem.* **258**, 3961 (1983).
6. E. Balzi, M. Choder, W. N. Chen, A. Varshavsky, A. Goffeau, *J. Biol. Chem.* **265**, 7464 (1990).
7. C. C. L. Wong *et al.*, *PLoS Biol.* **5**, e258 (2007).
8. M. Karakozova *et al.*, *Science* **313**, 192 (2006); published online 22 June 2006 (10.1126/science.1129344).
9. A. Varshavsky, *Cell* **69**, 725 (1992).
10. Materials and methods are available as supporting material on *Science* Online.
11. G. Kramer, D. Boehringer, N. Ban, B. Bukau, *Nat. Struct. Mol. Biol.* **16**, 589 (2009).
12. A. C. Lopo, C. C. Lashbrook, J. W. Hershey, *Biochem. J.* **258**, 553 (1989).
13. A. A. Komar, T. Lesnik, C. Reiss, *FEBS Lett.* **462**, 387 (1999).
14. A. P. Grollman, *J. Biol. Chem.* **242**, 3226 (1967).
15. S. Elias, A. Ciechanover, *J. Biol. Chem.* **265**, 15511 (1990).
16. S. Ferber, A. Ciechanover, *Nature* **326**, 808 (1987).
17. F. van den Ent, L. A. Amos, J. Löwe, *Nature* **413**, 39 (2001).
18. A. L. Goldberg, *Nature* **426**, 895 (2003).
19. R. Rai, A. Kashina, *Proc. Natl. Acad. Sci. U.S.A.* **102**, 10123 (2005).
20. Y. T. Kwon, A. S. Kashina, A. Varshavsky, *Mol. Cell. Biol.* **19**, 182 (1999).
21. J. Vandekerckhove, K. Weber, *Arch. Int. Physiol. Biochim.* **86**, 891 (1978).
22. K. L. Redman, P. A. Rubenstein, *Methods Enzymol.* **106**, 179 (1984).
23. D. K. Gonda *et al.*, *J. Biol. Chem.* **264**, 16700 (1989).

24. We thank R. Dominguez for help with actin structure analysis and the preparation of fig. S15; D. Volgin for helpful suggestions on quantitative polymerase chain reaction; S. Fuchs, Y. Goldman, and J. M. Murray for helpful discussions; and S. Kurosaka for critical reading of the manuscript. This work was supported by NIH grant 5R01HL084419 and W. W. Smith Charitable Trust and Philip Morris Research Management Group awards to A.K. and by the Intramural Research Program of NIH, National Center for Biotechnology Information, to S.A.S.

Supporting Online Material

www.sciencemag.org/cgi/content/full/329/5998/1534/DC1
Materials and Methods
SOM Text 1 to 3
Figs. S1 to S26
Tables S1 and S2
References

30 April 2010; accepted 20 July 2010
10.1126/science.1191701

MiR-16 Targets the Serotonin Transporter: A New Facet for Adaptive Responses to Antidepressants

Anne Baudry,[1] Sophie Mouillet-Richard,[1] Benoît Schneider,[1] Jean-Marie Launay,[2,3]* Odile Kellermann[1]*

The serotonin transporter (SERT) ensures the recapture of serotonin and is the pharmacological target of selective serotonin reuptake inhibitor (SSRI) antidepressants. We show that SERT is a target of microRNA-16 (miR-16). miR-16 is expressed at higher levels in noradrenergic than in serotonergic cells; its reduction in noradrenergic neurons causes de novo SERT expression. In mice, chronic treatment with the SSRI fluoxetine (Prozac) increases miR-16 levels in serotonergic raphe nuclei, which reduces SERT expression. Further, raphe exposed to fluoxetine release the neurotrophic factor S100β, which acts on noradrenergic cells of the locus coeruleus. By decreasing miR-16, S100β turns on the expression of serotonergic functions in noradrenergic neurons. Based on pharmacological and behavioral data, we propose that miR-16 contributes to the therapeutic action of SSRI antidepressants in monoaminergic neurons.

Transporters selective for serotonin [5-hydroxytryptamine (5-HT)] (SERTs), noradrenaline (NETs), or dopamine ensure the reuptake of monoamines at the synaptic cleft and thereby sustain the action of therapeutic agents in the treatment of a variety of psychiatric disorders (*1*). Dysfunction of serotonergic neurotransmission has been implicated in depression as well as obsessive-compulsive disorder, anxiety, and suicidal behavior (*2*). Selective serotonin reuptake inhibitors (SSRIs) are beneficial in the treatment of all these neuropsychiatric conditions. A still enigmatic observation is that SSRIs need to be administered for long time periods to yield clinical improvement (*3*).

The distribution of SERT in the brain mirrors that of serotonergic neuronal cell bodies and innervating fibers (*4*, *5*). Serotonergic raphe neurons project to most parts of the central nervous system and coordinate the physiology of the whole brain (*2*). Chronic SSRI antidepressant treatment promotes reductions in SERT binding and protein levels but does not affect SERT mRNA levels (*6*), suggesting that SSRIs may interfere with SERT translation. This control of translation could be exerted by microRNAs (miRNAs), which have emerged as crucial modulators of gene expression (*7*, *8*). Although the roles of miRNAs in cell fate decision, differentiation, maintenance of cell identity, survival, and neuronal plasticity are being uncovered (*9*, *10*), their targets remain largely unknown.

To investigate whether miRNAs provide a mechanism for adaptive changes in SERT expression in monoaminergic neurons, we first exploited the 1C11 neuroectodermal cell line, which can differentiate into either serotonergic ($1C11^{5\text{-HT}}$) or noradrenergic ($1C11^{NE}$) neuronal cells (fig. S1A) (*11*). 1C11 neuroectodermal cells express transcripts encoding SERT and neurotransmitter-related markers before their choice of cell fate (Fig. 1A and fig. S1B). Because these transcripts remain at roughly constant levels during serotonergic or noradrenergic differentiation, miRNAs may participate in the posttranscriptional mechanisms that prevent illegitimate mRNA translation according to each program.

Using in silico computational target prediction, we identified miR-16 as a miRNA with complementarity to the 3′ untranslated region of the SERT mRNA (fig. S2A) and then validated miR-16 as a SERT-targeting miRNA with a luciferase assay (fig. S2B). Consistent with a putative role of miR-16 as a negative regulator of SERT

[1]Cellules Souches, Signalisation et Prions, INSERM U747, Université Paris Descartes, 75006 Paris, France. [2]Pharma Research Department, F. Hoffmann-La-Roche, CH-4070 Basel, Switzerland. [3]Assistance Publique–Hôpitaux de Paris Service de Biochimie, RTRS Santé Mentale, U942 INSERM Hôpital Lariboisière, Paris, France.

*To whom correspondence should be addressed. E-mail: jean-marie.launay@lrb.aphp.fr (J.-M.L.); odile.kellermann@parisdescartes.fr (O.K.)

translation, we found that 1C11 neuroectodermal cells expressed a low level of miR-16, which increased along the noradrenergic pathway, whereas the level did not vary along the serotonergic program (fig. S2C).

If the SERT is indeed a target of miR-16, then miR-16 overexpression in 1C11$^{5\text{-HT}}$ cells should decrease SERT protein levels. During serotonergic differentiation, SERT translation starts at day 2 (*12*). Functional 5-HT uptake and antidepressant recognition occur at day 4. Among monoamine transporters, only SERT has the capacity to bind SSRI antidepressants [such as paroxetine and fluoxetine (Prozac)] (*13*). The SERT further recognizes the cocaine congener [^{125}I]-RTI-55, which also binds to NET (*12*). Using these pharmacological tools, we quantified the level of SERT expression in 1C11$^{5\text{-HT}}$ cells after transfection with miR-16. miR-16 overexpression reduced the number of [^{3}H]-paroxetine or [^{125}I]-RTI-55 binding sites by 40% (Fig. 1B). In contrast, the number of [^{3}H]-paroxetine and [^{125}I]-RTI-55 binding sites remained unchanged when 1C11$^{5\text{-HT}}$ cells were transfected with miR antisense oligonucleotides (anti–miR-16) (Fig. 1B), suggesting that SERT translation is insensitive to the endogenous basal level of miR-16 in 1C11$^{5\text{-HT}}$ cells.

1C11^{NE} noradrenergic cells selectively implement a functional NET at day 12 of their program (*11*). Although they express SERT mRNAs, SERT molecules are undetectable (Fig. 1, A and D). Assuming that the up-regulation of miR-16 during noradrenergic differentiation (fig. S2C) may have a role in silencing SERT transcripts, we exposed 1C11^{NE} cells to anti–miR-16. Binding was measured with three drugs: [^{3}H]-nisoxetine,

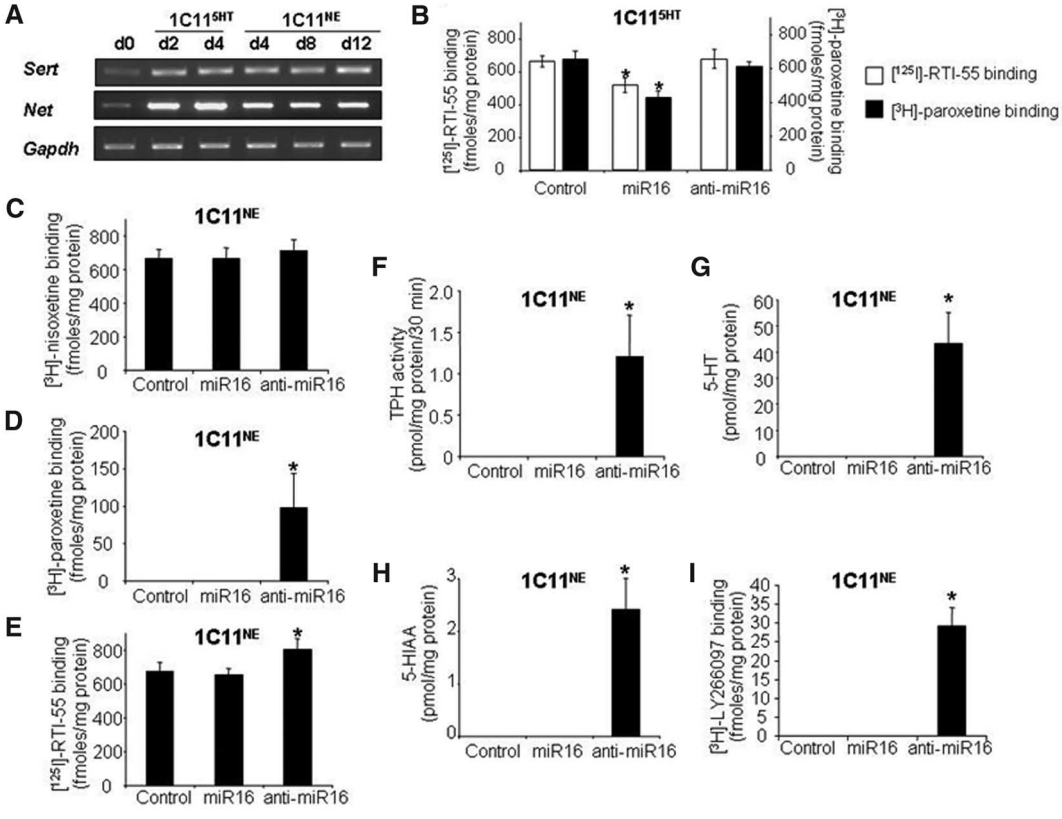

Fig. 1. miR-16 targets SERT in the 1C11 cell line. (**A**) Reverse transcription polymerase chain reaction (PCR) analysis of SERT and NET transcripts during serotonergic and noradrenergic differentiation. Glyceraldehyde phosphate dehydrogenase mRNA was used as a control. (**B**) Overexpression of miR-16 in 1C11$^{5\text{-HT}}$ cells reduces SERT expression. The level of SERT was determined by [^{125}I]-RTI-55 and [^{3}H]-paroxetine binding in 1C11$^{5\text{-HT}}$ day 4 cells untreated (control) or treated with miR-16 or anti–miR-16 at day 2 of serotonergic differentiation. (**C** to **E**) miR-16 reduction in 1C11^{NE} cells induces SERT expression and SSRI antidepressant binding, while not affecting NET expression. 1C11^{NE} cells were treated with miR-16 or anti–miR-16 at day 10 of the noradrenergic program. At day 12, NET and SERT expression were measured in cell homogenates using (C) [^{3}H]-nisoxetine, a selective inhibitor of noradrenaline uptake; (D) [^{3}H]-paroxetine, a selective inhibitor of 5-HT uptake; and (E) [^{125}I]-RTI-55, which recognizes NET and SERT. (**F** to **I**) miR-16 reduction in 1C11^{NE} cells unlocks the expression of serotonergic markers. Cell extracts from 1C11^{NE} day 12 cells untreated (control) or treated with miR-16 or anti–miR-16 at day 10 of differentiation were used to assess (F) TPH activity, (G) 5-HT intracellular content, (H) 5-hydroxyindoleacetic acid (5-HIAA) concentration, and (I) the amount of 5-HT$_{2B}$ receptors ([^{3}H]-LY 266097 binding). Data are means ± SEM of seven independent experiments, (B) *P < 0.01 versus control, (E) *P < 0.01, and [(D) and (F) to (I)] *P < 0.001 versus control and miR-16.

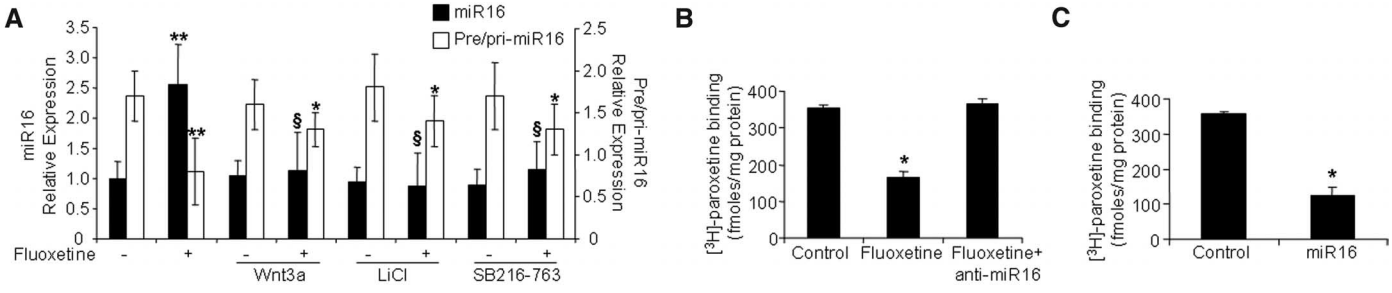

Fig. 2. Fluoxetine increases miR-16 levels in raphe by antagonizing canonical Wnt signaling. (**A**) Mice received chronic stereotaxic injection (2 μl/min) of fluoxetine (1 μM) into raphe for 3 days in combination or not with activators of the canonical Wnt pathway [Wnt3a (50 ng/ml), LiCl (1 mM), or SB-216763, a selective GSK-3β inhibitor (100 nM)]. The levels of miR-16 and pre/pri–miR-16 in raphe were determined by real-time PCR. Data are means ± SEM (n = 7 animals), **P < 0.01 versus control, *P < 0.05, and §P < 0.01 versus fluoxetine alone. (**B** and **C**) SERT expression ([^{3}H]-paroxetine binding) was determined in raphe extracts of mice perfused (2 μl/min) for 3 days into the raphe with fluoxetine (1 μM) in the presence or absence of anti–miR-16 (1 μl, 2 μM) (B) or after direct injection of miR-16 (1 μl, 2 μM) (C). Data are means ± SEM of seven animals, *P < 0.01 versus control.

which is selective for NET; [^{125}I]-RTI-55, which binds NET and SERT; and [^{3}H]-paroxetine, which recognizes SERT only. NET expression was insensitive to a reduction of miR-16 (Fig. 1C). In contrast, anti–miR-16 induced the appearance of paroxetine binding sites in 1C11^{NE} cells (Fig. 1D) and increased the number of RTI binding sites to the sum of nisoxetine and paroxetine binding sites (Fig. 1E). The number of newly induced RTI sites equaled the number of paroxetine binding sites and may thus be ascribed to de novo expressed SERT molecules. Hence, the inhibition of miR-16 unlocks SERT protein expression in 1C11^{NE} cells and renders noradrenergic cells competent to recognize SSRI antidepressants.

Next, we investigated whether decreasing miR-16 levels in 1C11^{NE} cells would promote changes in noradrenergic phenotypic parameters distinct from NET and/or allow the implementation of serotonergic functions, in addition to that of SERT. Neutralization of endogenous miR-16 with anti–miR-16 had no impact on noradrenergic-associated functions in 1C11^{NE} cells (fig. S3). In contrast, the cells acquired a complete serotonergic metabolism, as defined by the ability to synthesize, store, and degrade 5-HT, and they expressed 5-HT$_{2B}$ receptors (Fig. 1, F to I). These results show that miR-16 acts as a global repressor of the expression of serotonergic-specific functions in 1C11^{NE} cells.

We hypothesized that the miR-16–dependent regulation of the SERT shown in the 1C11 cell line may have physiopathological relevance in vivo. We first quantified miR-16 in mouse serotonergic raphe nuclei (*2*) versus the noradrenergic locus coeruleus (*14*). As in the 1C11 cell line, lower levels of miR-16 were found in raphe than in the locus coeruleus (fig. S2D). Then we assessed whether SSRI antidepressant treatment could alter the levels of miR-16 in these regions of the mouse brain. When fluoxetine was infused into raphe, we observed a 2.5-fold increase in the level of miR-16 and a twofold reduction in [^{3}H]-paroxetine binding in raphe (Fig. 2, A and B). Direct injection of miR-16 into raphe yielded a similar decrease in [^{3}H]-paroxetine binding (Fig. 2C). Finally, [^{3}H]-paroxetine binding was not affected after the infusion of fluoxetine together with anti–miR-16 (Fig. 2B). These data demonstrate that fluoxetine regulates SERT expression through miR-16 in raphe.

The fluoxetine-induced up-regulation of miR-16 in raphe nuclei may involve a pre/pri–miR-16 enhanced transcription and/or maturation. In raphe versus the locus coeruleus, the level of pre/pri–miR-16 was inversely correlated with the level of miR-16 (compare figs. S2D and S4). In addition, the fluoxetine-mediated increase in miR-16 in raphe was accompanied by a decrease in pre/pri–miR-16 (Fig. 2A), thus supporting the maturation hypothesis. Because canonical Wnt signaling may repress miR-16 maturation (*15*), we quantified the levels of miR-16 and pre/pri–miR-16 under combined fluoxetine treatment and activation of the Wnt pathway. The up-regulation of miR-16 and the down-regulation of pre/pri–miR-16 triggered by fluoxetine in raphe were both eliminated by either Wnt3a, LiCl, or SB-216763 (Fig. 2A). Chronic fluoxetine treatment actually interfered with canonical Wnt signaling, as inferred from the increase in glycogen synthase kinase–3β (GSK-3β) activity (fig. S5A). Hence, the SSRI fluoxetine augments the level of miR-16 in raphe by antagonizing Wnt signaling and thereby negatively regulates SERT expression.

When infused into the locus coeruleus, fluoxetine failed to induce any change in miR-16 expression (fig. S6), which is in agreement with the lack of SERT expression in noradrenergic neurons under basal conditions. In contrast, upon infusion of fluoxetine into raphe, we monitored a 30% reduction in miR-16 in the locus coeruleus (Fig. 3A), associated with a decrease in GSK3β activity (fig. S5B). This down-regulation of miR-16 was accompanied by the induction of SERT expression, as well as tryptophan hydroxylase

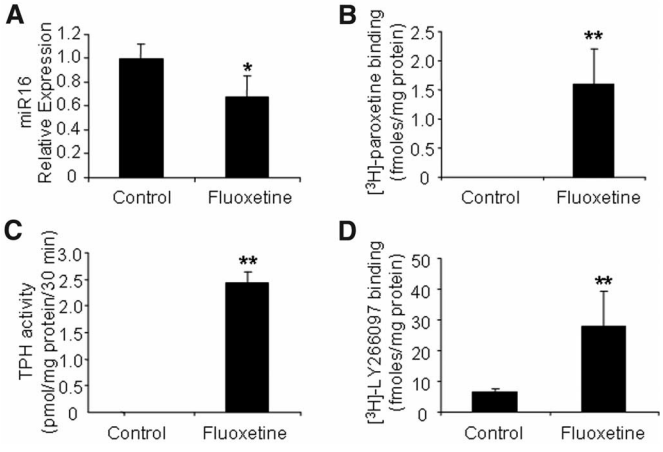

Fig. 3. Fluoxetine injection into raphe decreases miR-16 in the locus coeruleus and turns on SERT expression, 5-HT synthesis, and 5-HT$_{2B}$ receptor expression in the locus coeruleus. Chronic stereotaxic injection of fluoxetine (1 μM, 2 μl/min) into the mouse raphe was carried out for 3 days. All measurements were made on locus coeruleus extracts: (**A**) miR-16 level using real-time PCR, (**B**) SERT expression ([^{3}H]-paroxetine binding), (**C**) TPH activity, and (**D**) amount of 5-HT$_{2B}$ receptors ([^{3}H]-LY 266097 binding). Values are means ± SEM of seven animals, *P < 0.01 and **P < 0.001 versus control.

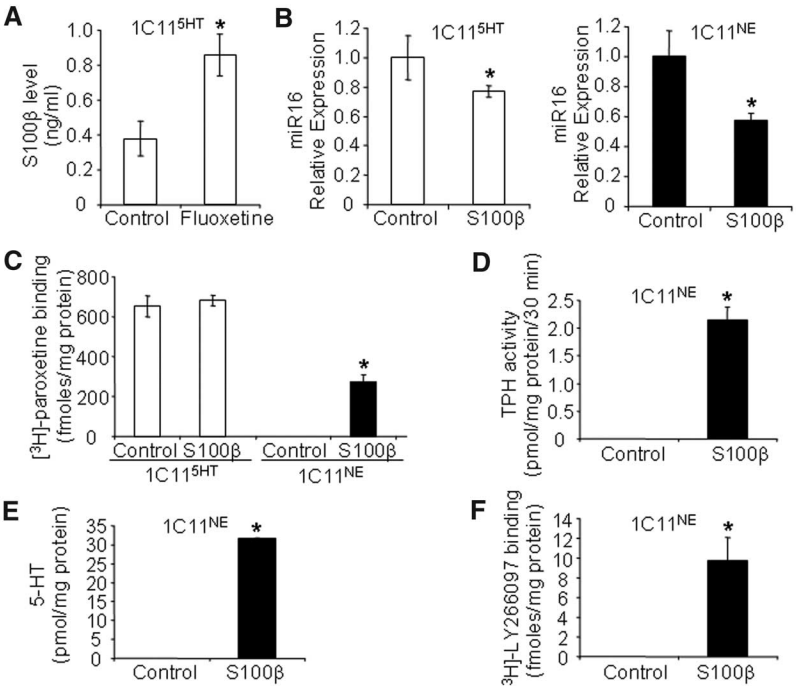

Fig. 4. Fluoxetine induces 1C11$^{5\text{-}HT}$ cells to release S100β, which decreases miR-16 expression and triggers the implementation of serotonergic markers in 1C11^{NE} cells. (**A**) Treatment of 1C11$^{5\text{-}HT}$ cells with fluoxetine (50 nM) for 2 days increased the extracellular content of S100β. (**B** to **F**) 1C11$^{5\text{-}HT}$ or 1C11^{NE} cells were exposed to S100β (1 nM) for 2 days. (B) The level of miR-16 as analyzed by real-time PCR was decreased in 1C11$^{5\text{-}HT}$ and 1C11^{NE} cells. (C) S100β did not affect SERT expression in 1C11$^{5\text{-}HT}$ cells, whereas it induced the expression of SERT in 1C11^{NE} cells ([^{3}H]-paroxetine binding). In 1C11^{NE} cells, S100β triggered de novo 5-HT synthesis (detection of TPH activity) (D), 5-HT intracellular content (E), and 5-HT$_{2B}$ receptor expression ([^{3}H]-LY 266097 binding) (F). Data are means ± SEM of seven independent experiments, *P < 0.01 versus control.

(TPH) activity and 5-HT_{2B} receptors (Fig. 3, B to D). Confocal microscopy confirmed that SERT induction occurred in tyrosine hydroxylase–positive neurons (fig. S7). Thus, the locus coeruleus responds to fluoxetine injection in raphe by switching on serotonergic functions. Likewise, in a more clinically relevant paradigm, 20 days after daily intraperitoneal injection of fluoxetine into mice, we measured a 27% decrease of miR-16 associated with an expression of SERT molecules in the locus coeruleus (fig. S8, A and B).

The question then arises of how the response of serotonergic neurons to fluoxetine treatment is relayed to noradrenergic neurons in vivo. Reciprocal connections exist between these two brainstem monoaminergic nuclei, thus supporting communication between the two systems (*16*). Recently, the expression of miR-16 in monocytes was shown to be down-regulated by S100β (*17*), a neurotrophic protein that is up-regulated by fluoxetine treatment (*18*). We therefore hypothesized that the secretion of S100β increases upon exposure of raphe to fluoxetine and that this protein acts as a paracrine factor to promote the reduction in miR-16 in the locus coeruleus, in turn unlocking the expression of serotonergic functions. We first exposed $1C11^{5\text{-}HT}$ cells to fluoxetine and observed an accumulation of S100β in the culture medium (Fig. 4A). Although the addition of S100β slightly decreased miR-16 levels in these serotonergic cells (Fig. 4B), it did not affect SERT expression (Fig. 4C), which is in agreement with the lack of impact of miR-16 silencing on SERT in $1C11^{5\text{-}HT}$ cells (Fig. 1B). A larger decrease (43% of control level) of miR-16 was seen in $1C11^{NE}$ cells exposed to S100β (Fig. 4B), which correlated with the appearance of SERT (Fig. 4C). In addition, after S100β treatment, $1C11^{NE}$ cells acquired the ability to synthesize and store 5-HT (Fig. 4, D and E) and to express 5-HT_{2B} receptors (Fig. 4F). These data thus validate our working hypothesis on an in vitro level. We then measured the level of S100β in raphe upon infusion of fluoxetine. Fluoxetine up-regulated S100β levels in serotonergic nuclei (133% versus control) (Fig. 5A). Further, injection of S100β into the locus coeruleus decreased (by 22.4%) miR-16 levels and turned on the expression of SERT (Fig. 5, B and C). Finally, antibody-mediated neutralization of S100β in the locus coeruleus prevented the decrease in miR-16 levels observed upon infusion of fluoxetine in raphe (Fig. 5D). In addition, the decrease in miR-16 and the onset of SERT expression observed in the locus coeruleus, upon systemic fluoxetine treatment, were both eliminated by small interfering RNA–mediated knockdown of S100β in raphe (fig. S8, A and B). The data from $1C11^{5\text{-}HT}$ cells (Fig. 4A) and the innervation of the locus coeruleus by raphe fibers (*16*) strengthen the hypothesis that secretion of S100β by serotonergic neurons, at the locus coeruleus, mediates the action of fluoxetine. Secretion of S100β by glial cells in the raphe is less likely to promote a long-range action on the locus coeruleus.

Finally, we demonstrated the potential benefit of the fluoxetine-induced regulation of miR-16 in two mouse models of depression: the forced swimming test (FST) (fig. S9) and the unpredictable chronic mild stress (UCMS) paradigm (*19*, *20*). Mice exposed to a 6-week UCMS regimen exhibited a deterioration of coat state and reductions in body weight gain, sucrose preference, and locomotor activity that were alleviated to the same extent either by chronic infusion of fluoxetine or miR-16 into raphe or by anti–miR-16 into the locus coeruleus (Fig. 5, E to H) (*21*).

Our study identifies the SERT-targeting miRNA miR-16 as a player in relaying SSRI antidepressant action (fig. S10). Fluoxetine operates directly on serotonergic raphe nuclei by

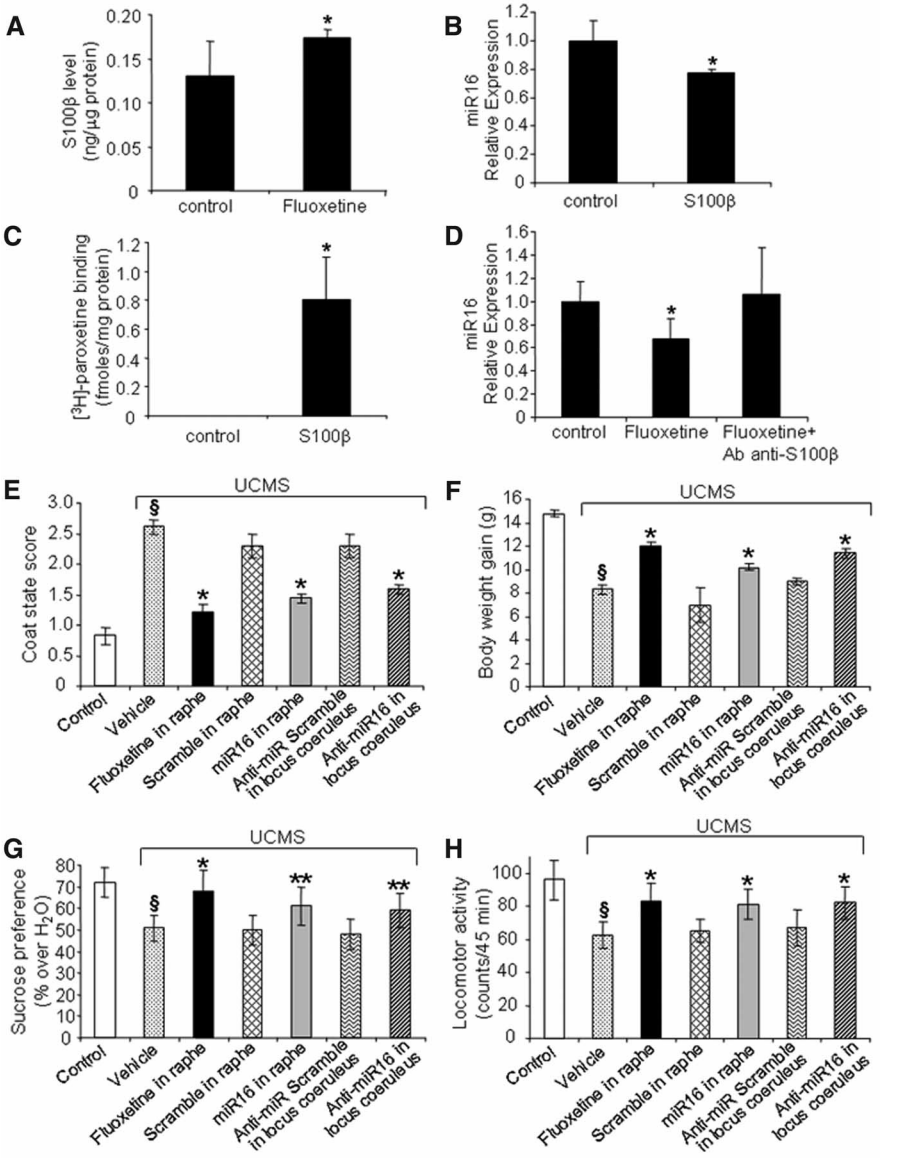

Fig. 5. Fluoxetine injection into raphe acts on the locus coeruleus via S100β and induces behavioral responses that are mimicked by increases in miR-16 in raphe or decreases in miR-16 in the locus coeruleus. (**A**) Chronic stereotaxic injection of fluoxetine (1 μM, 2 μl/min, 3 days) into mouse raphe induced S100β efflux. (**B** and **C**) Stereotaxic injection of S100β (1 nM, 2 μl/min, 1 day) into the mouse locus coeruleus decreased miR-16 (B) and induced SERT expression (C) in locus coeruleus extracts as determined by real-time PCR and [^{3}H]-paroxetine binding, respectively. (**D**) Injection of antibodies against S100β (1 μg/ml, 24 hours) into the locus coeruleus prevented the down-regulation of miR-16 in this brain structure induced by chronic infusion of fluoxetine into raphe. Data are means ± SEM ($n = 7$ animals), *$P <$ 0.01 versus control. (**E** to **H**) Six-week UCMS-induced deterioration of the coat state score (E), reduction of body weight gain (F), and decreases in sucrose preference (G) and locomotor activity (H) were alleviated by stereotaxic injection of fluoxetine (1 μM, 2 μl/min, in the last 5 weeks) or miR-16 (1 μl, 2 μM, every 36 hours) into mouse raphe or anti–miR-16 (1 μl, 2 μM, every 36 hours) into the locus coeruleus. The injection of scrambled miRNAs did not yield any improvement in these tests. Data are means ± SEM ($n = 6$ to 9 mice per group). §$P <$ 0.01 versus control, *$P <$ 0.05, and **$P <$ 0.01 versus vehicle UCMS.

increasing the maturation of miR-16 from its precursor pre/pri–miR-16. Raphe additionally responds to chronic fluoxetine treatment by releasing S100β, which in turn acts on the noradrenergic neurons of the locus coeruleus. By lowering miR-16 levels, S100β unlocks the expression of serotonergic functions in this noradrenergic brain area. Our pharmacological and behavioral data thus posit miR-16 as a central effector that regulates SERT expression and mediates the adaptive response of serotonergic and noradrenergic neurons to fluoxetine treatment.

References and Notes

1. G. E. Torres, R. R. Gainetdinov, M. G. Caron, *Nat. Rev. Neurosci.* **4**, 13 (2003).
2. E. C. Azmitia, *Int. Rev. Neurobiol.* **77**, 31 (2007).
3. O. Berton, E. J. Nestler, *Nat. Rev. Neurosci.* **7**, 137 (2006).
4. Y. Qian, H. E. Melikian, D. B. Rye, A. I. Levey, R. D. Blakely, *J. Neurosci.* **15**, 1261 (1995).
5. D. L. Murphy *et al.*, *Neuropharmacology* **55**, 932 (2008).
6. S. Benmansour, W. A. Owens, M. Cecchi, D. A. Morilak, A. Frazer, *J. Neurosci.* **22**, 6766 (2002).
7. D. P. Bartel, *Cell* **136**, 215 (2009).
8. C. M. Croce, *Nat. Rev. Genet.* **10**, 704 (2009).
9. K. S. Kosik, *Nat. Rev. Neurosci.* **7**, 911 (2006).
10. V. K. Gangaraju, H. Lin, *Nat. Rev. Mol. Cell Biol.* **10**, 116 (2009).
11. S. Mouillet-Richard *et al.*, *J. Biol. Chem.* **275**, 9186 (2000).
12. J. M. Launay, B. Schneider, S. Loric, M. Da Prada, O. Kellermann, *FASEB J.* **20**, 1843 (2006).
13. A. Frazer, *J. Clin. Psychopharmacol.* **17** (suppl. 1), 2S (1997).
14. E. J. Nestler, M. Alreja, G. K. Aghajanian, *Biol. Psychiatry* **46**, 1131 (1999).
15. G. Martello *et al.*, *Nature* **449**, 183 (2007).
16. M. A. Kim, H. S. Lee, B. Y. Lee, B. D. Waterhouse, *Brain Res.* **1026**, 56 (2004).
17. N. Shanmugam, M. A. Reddy, R. Natarajan, *J. Biol. Chem.* **283**, 36221 (2008).
18. R. Manev, T. Uz, H. Manev, *Eur. J. Pharmacol.* **420**, R1 (2001).
19. A. Surget *et al.*, *Neuropsychopharmacology* **34**, 1363 (2009).
20. P. Willner, *Psychopharmacology (Berlin)* **134**, 319 (1997).

21. Materials and methods and supporting data are available on *Science* Online.

22. We thank P. Weil-Malherbe, V. Mutel, F. d'Agostini, G. Zürcher, E. Borroni, J. L. Moreau, F. Jenck, M. Bühler, and N. Pieron for skillful methodological assistance, and S. Blanquet, M. Briley, and L. Aggerbeck for critical reading of the manuscript. O.K. is a professor at Paris XI University. This work was funded by CNRS, ANR, and INSERM.

Supporting Online Material

www.sciencemag.org/cgi/content/full/329/5998/1537/DC1
Materials and Methods
Figs. S1 to S10
References

14 June 2010; accepted 4 August 2010
10.1126/science.1193692

Relating Introspective Accuracy to Individual Differences in Brain Structure

Stephen M. Fleming,[1]*† Rimona S. Weil,[1,2]* Zoltan Nagy,[1] Raymond J. Dolan,[1] Geraint Rees[1,2]

The ability to introspect about self-performance is key to human subjective experience, but the neuroanatomical basis of this ability is unknown. Such accurate introspection requires discriminating correct decisions from incorrect ones, a capacity that varies substantially across individuals. We dissociated variation in introspective ability from objective performance in a simple perceptual-decision task, allowing us to determine whether this interindividual variability was associated with a distinct neural basis. We show that introspective ability is correlated with gray matter volume in the anterior prefrontal cortex, a region that shows marked evolutionary development in humans. Moreover, interindividual variation in introspective ability is also correlated with white-matter microstructure connected with this area of the prefrontal cortex. Our findings point to a focal neuroanatomical substrate for introspective ability, a substrate distinct from that supporting primary perception.

Our moment-to-moment judgments of the outside world are often subject to introspective interrogation. In this context, introspective or "metacognitive" sensitivity refers to the ability to discriminate correct from incorrect perceptual decisions (*1*), and its accuracy is essential for the appropriate guidance of decision-making and action (*2*, *3*). For example, low confidence that a recent decision was correct may prompt us to reexamine the evidence or seek a second opinion. Recently, behavioral studies have begun to quantify metacognitive accuracy following simple perceptual decisions and to isolate variations in this ability: A decision may be made poorly, yet an individual may believe that his or her performance was good, or vice versa (*4*–*8*). Whereas previous work has investigated how confidence in perceptual decisions varies from trial to trial (*9*, *10*), little is known about the biological basis of metacognitive ability, defined here as how well an individual's confidence ratings discriminate correct from incorrect decisions over time. We hypothesized that individual differences in metacognitive ability would be reflected in the anatomy of brain regions responsible for this function, in line with similar associations between brain anatomy and performance in other cognitive domains (*11*–*15*).

We objectively quantified variability in metacognitive sensitivity between individuals and then related these interindividual differences to brain structure measured with magnetic resonance imaging (MRI). This approach was motivated by observations that individual differences in a range of skills—such as language (*11*), decision-making (*12*), and memory (*13*)—are consistently associated with variation in healthy brain anatomy. Our experimental design dissociated a quantitative measure of metacognitive accuracy, A_{roc} (which is specific to an individual), from both objective task performance and subjective confidence (which both vary on a trial-by-trial basis). Earlier patient studies describe candidate brain regions in which damage is associated with poor introspective ability: in particular, a prefrontal-parietal network (*16*–*18*). Theories of prefrontal

[1]Wellcome Trust Centre for Neuroimaging, University College London, 12 Queen Square, London WC1N 3BG, UK. [2]Institute of Cognitive Neuroscience, University College London, 17 Queen Square, London WC1N 3AR, UK.

*These authors contributed equally to this work.
†To whom correspondence should be addressed. E-mail: s.fleming@fil.ion.ucl.ac.uk

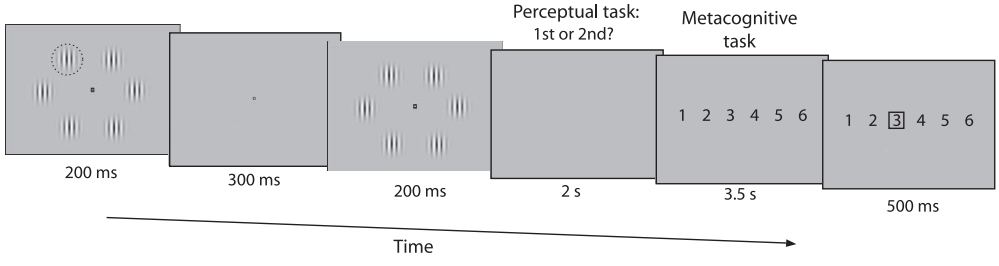

Fig. 1. Behavioral task. Participants completed a two-alternative forced-choice task that required two judgments per trial: a perceptual response followed by an estimate of relative confidence in their decision. The perceptual response indicated whether the first or second temporal interval contained the higher-contrast (pop-out) Gabor patch (highlighted here with a dashed circle that was not present in the actual display), which could appear at any one of six locations around a central fixation point. Pop-out Gabor contrast was continually adjusted with the use of a staircase procedure to maintain ~71% performance. Confidence ratings were made using a one-to-six scale, with participants encouraged to use the whole scale from one = low relative confidence to six = high relative confidence. The black square in the rightmost panel indicates the choice made in the metacognitive task.